Artificial Enzymes

International Edition: DOI: 10.1002/anie.201708036
German Edition: DOI: 10.1002/ange.201708036

Switchable Hydrolase Based on Reversible Formation of Supramolecular Catalytic Site Using a Self-Assembling Peptide

Chunqiu Zhang, Ramim Shafi, Ayala Lampel, Douglas MacPherson, Charalampos G. Pappas, Vishal Narang, Tong Wang, Charles Maldarelli, and Rein V. Ulijn**

Abstract: *The reversible regulation of catalytic activity is a feature found in natural enzymes which is not commonly observed in artificial catalytic systems. Here, we fabricate an artificial hydrolase with pH-switchable activity, achieved by introducing a catalytic histidine residue at the terminus of a pH-responsive peptide. The peptide exhibits a conformational transition from random coil to β-sheet by changing the pH from acidic to alkaline. The β-sheet self-assembles to form long fibrils with the hydrophobic edge and histidine residues extending in an ordered array as the catalytic microenvironment, which shows significant esterase activity. Catalytic activity can be reversible switched by pH-induced assembly/disassembly of the fibrils into random coils. At higher concentrations, the peptide forms a hydrogel which is also catalytically active and maintains its reversible (de-)activation.*

The control of catalytic activity is important in the regulation of biological processes including metabolism, signal transduction, differentiation and cell growth.[1] The catalytic activity of natural enzymes is regulated by physicochemical stimuli, for example, small binding ligands, light, temperature, and pH.[2] In natural enzymes the conversion of substrate to product occurs within the microenvironment of a catalytic site formed by the enzyme's secondary and tertiary structure, within which the substrate binds to chemical moieties and is brought into contact with surrounding catalytic functional groups that carry out the transformation. External stimuli can act to reconfigure this arrangement by inducing changes in the conformation at the site.

[*] Dr. C. Zhang, R. Shafi, Dr. A. Lampel, D. MacPherson, Dr. C. G. Pappas, Dr. V. Narang, Dr. T. Wang, Prof. R. V. Ulijn
Advanced Research Science Center, ASRC, at the Graduate Center, The City University of New York
85 St. Nicholas Terrace, New York, NY 10031 (USA)
E-mail: Rein.Ulijn@asrc.cuny.edu
Prof. R. V. Ulijn
Department of Chemistry & Biochemistry, Hunter College
695 Park Ave., New York, NY 10065 (USA),
and
Ph.D. programs in Chemistry and Biochemistry, The Graduate Center of CUNY, 365 Fifth Avenue, New York, NY 10016 (USA)
Dr. C. Zhang, Prof. C. Maldarelli
Chemical Engineering Department, The City University of New York
160 Convent Avenue, New York, NY 10031 (USA)
E-mail: cmaldarelli@ccny.cuny.edu
Supporting information and the ORCID identification number(s) for the author(s) of this article can be found under https://doi.org/10.1002/anie.201708036.

Incorporating the stimuli-responsive behavior of natural enzymes in artificial ones may enable control of reaction pathways for applications, but is challenging as it requires the integration of stimuli-responsiveness with binding and precise positioning of catalytic moieties. Genetic engineering and directed evolution methods can be used to mutate existing stimuli-responsive proteins with active catalytic centers to form allosteric enzymes.[3] Alternatively, stimuli-responsive groups can be grafted to existing natural enzymes to obtain hybrids with enzymatic switchable behavior.[4] Synthetic, de novo constructed switchable catalysts have been developed in which stimuli directly reconfigure the active site on a catalytic small molecule to effect a transition from the inactive to the active form.[5]

Supramolecular assemblies are of interest for de novo construction of switchable catalysts because these structures allow for a precise tailoring of a catalytic microenvironment. In addition, supramolecular assemblies enable incorporation of features not seen in natural enzymes, such as the incorporation of arrays of numerous active sites into each nanostructure, potentially enhancing catalytic activity due to cooperativity. In addition, there is scope for the introduction of multiple, synergistic catalytic sites into a single nanostructure. The use of peptides has the advantage that the known catalytic activities of amino acid residues in natural enzymes can be incorporated into the artificial construct. Indeed, functioning artificial biocatalysts from self-assembled peptides have been developed using a range of designs,[6,7] including α-helical coiled-coils,[6a] peptide amphiphiles,[7a] short β-sheet forming peptides,[6b,f,7b,f] aromatic peptide amphiphiles,[7c] tripeptide assemblies,[7d] and bola-type amphiphiles.[7e] These systems typically incorporate one (or more) histidine and/or other residues relevant to catalysis or binding, sometimes including metal ions to assist folding and catalysis. Remarkably, in hydrolysis of activated esters, a typical model reaction for hydrolases, the catalytic efficiencies obtained for these peptide-based supramolecular catalysts have been broadly similar, and are still several orders of magnitude below the activities of natural enzymes.[8]

Here we focus on developing an artificial switchable enzyme using amphiphilic self-assembling peptides with pH control, by reversible formation of an active site (i.e. the switch aligns a binding region with the catalytic residues). To integrate stimuli-responsive behavior in these self-assembled structures, the assembly (or a re-assembly from an inactive form) is required to be triggered by a physicochemical cue. Only very recent research had begun to incorporate supramolecular switches by using selenide residues for redox control.[6e] Our starting point is based on the family of self-

assembling peptides developed by Schneider and Pochan (the so-called MAX series) that are typically composed of two strands of beta-sheet forming valine–lysine (VK) repeats connected via a D-proline, proline–threonine (^{D}PPT) turn sequence.[9] MAX peptides have shown the ability to self-assemble into well-defined fibrils and hydrogels, depending on their conformation transition from unfolded to folded state triggered by external stimuli (typically, changes in pH or ionic strength). Of the available peptide self-assembly approaches, the MAX systems are among the best characterized systems, which combine stimuli-responsiveness and precise, in register assembly of peptide chains.[9c–e] They therefore provide a suitable model system for the formation of stimuli-responsive catalytic materials that rely on reversible alignment of a binding site with catalytic residues.

Our design is a modification of MAX1,[9e] which is composed of N- and C-terminal β-strands connected by a type II′ β-turn when the two strands come into hydrogen bonding registry to form a β-sheet (Figure 1 A), but in this

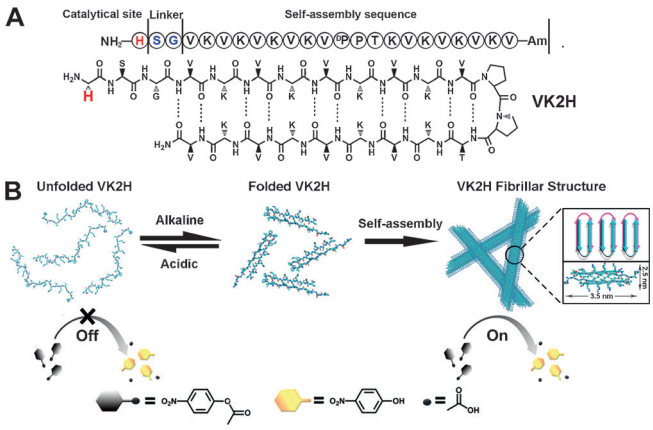

Figure 1. A) Chemical structure of peptide VK2H. B) Schematic representation of the pH-switched artificial hydrolase based on conformation change of VK2H and the cartoon structure of the bilayer.

case modified at the N-terminus with a HSG catalytic sequence, named VK2H (two strands of VK repeats, functionalized with H). At neutral pH, the lysine groups are protonated, and this causes a repulsion which prevents the hydrogen bonding of the strands of the hairpin, so that the peptide adopts a random coil configuration. Increasing the pH to 9 reduces this repulsion as the lysine groups deprotonate, and VK2H adopts a β-sheet configuration with the two strands in antiparallel conformation (Figure 1 B). The alternation of the valine and lysine in the backbone results in one face of the sheet being hydrophobic and the other one being hydrophilic. A second layer of hairpins causes formation of a bilayer with the hydrophobic faces of the two layers facing and buried into each other to separate the hydrophobic moieties from water.[10] Once the hairpin folds, VK2H self assembles laterally through hydrogen binding of the strands of adjoining hairpins to form fibrils. Both the self-assembly of fibrils and the consequent gelation are reversible with a decrease in pH causing a break-up into the random coiled form of the peptide.

The edge of the self-assembled fibrillar structure of VK2H, which is hydrophobic, provides a unique vantage point for the installation of a catalytic site. In particular, analogous to MAX peptides, the histidine residues along the fibrils are expected to be exposed to the solution,[9e] enabling interaction with the substrate. In addition, the hydrophobic valine face can function as a binding site for substrates with nonpolar groups, giving rise to a similar architecture to His-functionalized bola-amphiphiles reported previously,[7e] but with the added advantage of precise regulation in the formation of this multi-component active site. We use this design to construct an artificial hydrolase by appending to the N-terminus the catalytic residue histidine, and a spacer (serine and glycine) (VK2H). Here, as with these prior studies,[7] we use *p*-nitrophenyl acetate (pNPA) as the substrate; ester cleavage produces the chromogen *p*-nitrophenol and acetic acid (Figure 1 B). We first confirm the dynamic conformation change of VK2H upon changing pH. We then demonstrate significant catalytic activity when VK2H is self-assembled into fibrils. We also confirm the essential role of the histidine by replacing the histidine with glycine (VK2G), which also self-assembles into fibrils as VK2H but with much reduced catalytic activity. Futhermore, we studied VR2H, where lysine residues are replaced by arginine, which has a higher critical pH for assembly due to the higher pK_a of the arginines, in order to confirm the important role of supramolecular assembly in catalysis. Histidine amide is used as a soluble control for catalytic activity. Finally, we take advantage of the ability of the constructs to form hydrogels and demonstrate that VK2H forms hydrogels with switchable catalytic activity.

The peptides VK2H, VK2G and VR2H were synthesized using standard solid phase peptide synthesis, and their molecular weight was confirmed by MALDI-TOF MS or ESI MS (Figures S1–S3 in the Supporting Information). The conformational transition of VK2H from random coil to fibrils induced by an increase in pH involves the formation of extended β-sheet structures. As characteristic circular dichroism (CD) spectra for β-sheets exhibit a minimum around 216 nm,[10e,11] we measured the CD spectra as a function of pH of aqueous solutions (50 μM) of VK2H to confirm the conformational transition. As shown in Figure 2 A, with an

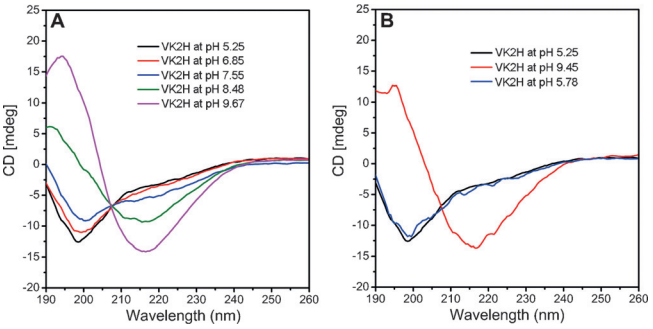

Figure 2. A) Circular dichroism spectra of peptide VK2H in solution (50 μM) at different pH ranging from 5.3 to 9.7. B) Circular dichroism spectra of the reversible transition of a diluted VK2H solution (50 μM) by regulating pH from 5.3 to 9.5 and then back to 5.8. The path length of the cuvette is 1 mm.

increase in pH from acidic to alkaline, the 216 minima became more pronounced, providing strong evidence for the transition from random coil to β-sheet, indicative of β-sheet formation. This data is in direct agreement with the pH dependent spectra of MAX1,[9] and confirms that the HSG sequence in VK2H does not alter the ability of the peptides to assemble into β-sheet conformations. For the VK2H construct to retain switchable catalytic behavior in response to pH, it is important that the conformational change is reversible, and in Figure 2B we provide evidence of this reversibility by at first increasing and then decreasing the pH of a VK2H solution, and recording the corresponding CD spectra. As shown in the Figure, the complete β-sheet conformation was triggered after the pH was regulated from 5.3 to 9.5, but then transferred back to the random coil conformation when the pH was changed to 5.8 again. These results confirmed that the VK2H was inherently pH-responsive, and the reversible conformation transition could be regulated by pH change. In addition, we also measured the CD spectra of the control VK2G as a function of pH (Figure S4) and found identical behavior to VK2H. As expected, because of the higher pK_a value of arginine versus lysine, the control peptide VR2H (Figure S5) shows a reduced β-sheets structure at pH 9.0 compared to VK2H, with a conformation transition occurring when the pH was increased to over 10.5.

Atomic force microscopy (AFM) was used to obtain direct evidence of the self-assembly of the VK2H hairpins into fibrils (Figure 3A) with relatively homogeneous feature heights of 2.5 nm. Assuming the VK2H fibrils adsorb with one of their hydrophilic faces down onto the hydrophilic mica surface, the observed height is consistent with estimates of the height of the hairpin bilayer formed by the collapsed of the hydrophobic valine groups (Figure 1B). Similar aligned fibril structures are observed for VK2G (Figure S6). Further insight into the fibrous form of the supramolecular assemblies of VK2H can be obtained by transmission electron microscopy (TEM) (Figure S7). The visualized fibrous structures are, as in the AFM images, hundreds of nanometers in length. Their widths are of the order of 3.5 nanometers, which are consistent with the hairpin width.

We found that VK2H and VK2G can form a mechanically rigid hydrogel matrix at higher concentrations due to fibrillar entanglement and crosslinking, and we measure an approximate value of 0.5 wt% percent (2.0 mM) for the minimum gelation concentration (MGC) using the inverted tube test for both peptides. The hydrogelation is reversible with change in the pH: Aqueous solution prepared above the MGC at pH 6.0 was transferred to gel when the pH is raised to 9.5 (see Figure 4A), and the incubation time for gelation is approximately 10 min. Addition of hydrochloric acid to reduce the pH back to 6.0 causes the gel to fluidize. To characterize the mechanical rigidity of the gel, the storage modulus G′ and loss modulus G″ are obtained for small oscillatory strain deformations of a prescribed frequency (linear viscoelastic regime) in a rheometer in a parallel plate geometry. As shown in Figure 4B and Figure S8, values of G′ and G″ are of order 10^3 and 10^2, respectively, and are nearly constant with frequency. The value (0.1) of the loss tangent G′/G″ and the constant value of G′ indicate a material that is solid-like, and the values of these moduli are in agreement with those measured for

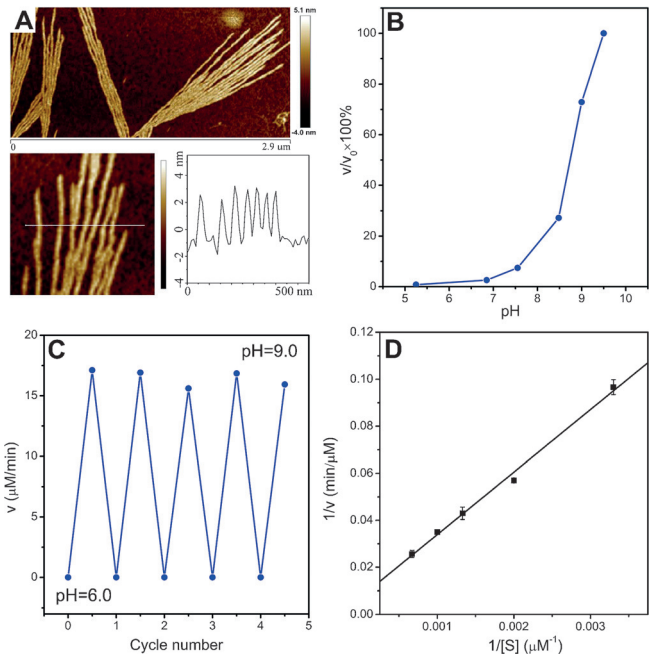

Figure 3. A) AFM images of VK2H nanofibers and height profile along the white line. B) Plot of initial catalytic rate (v) of VK2H nanofibers at different pH versus the initial catalytic rate of VK2H fibrils at pH 9.5. C) The on–off switch of catalytic activity of VK2H peptide by a change in pH between 6.0 and 9.0. D) Double-reciprocal plot of the hydrolysis of different concentration of pNPA under the catalysis of VK2H fibrils (32 μM).

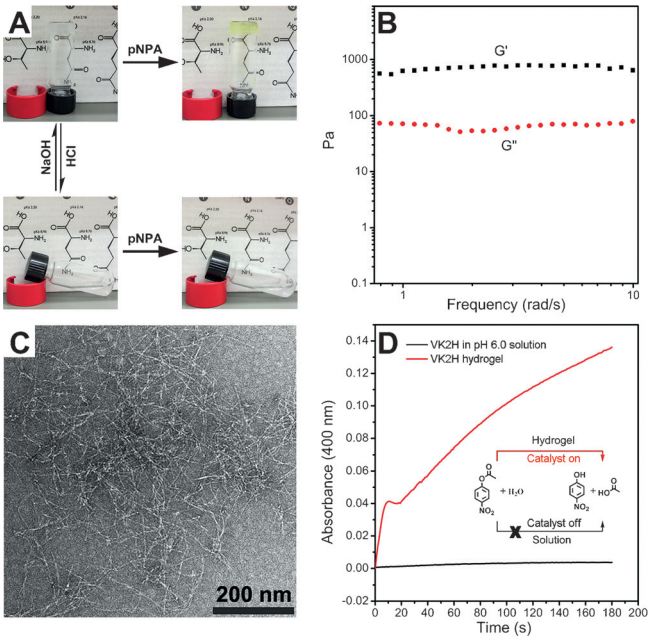

Figure 4. A) Optical images of the reversible transition process from solution to hydrogel by regulating the pH from 6.0 to 9.5 with VK2H peptide (4.0 mM) and the color change of hydrogel in the presence of pNPA. B) Frequency dependence of dynamic storage modulus (G′) and loss modulus (G″) of VK2H hydrogel with VK2H peptide (4.0 mM). C) Transmission electron microscope (TEM) image of VK2H hydrogel. D) Plots of absorbance vs. time for hydrolysis of pNPA (500 μM) in the presence of VK2H hydrogel at pH 9.5 or VK2H solution at pH 6.0.

MAX1.[9] The more extensive, elaborated network of the VK2H fibrils in the 1 wt% (4.0 mM) gel state (Figure 4C) observed by TEM is evident when compared to the structure in the 30 μM aqueous solution (Figure S7) and accounts for the solid-like nature.

The hydrolytic activity of VK2H in solution was measured at adjusted values for the solution pH. Reactions were carried out at different concentrations (8–32 μM, below the gelation point) with different substrate concentrations and adjusted pH values. The concentration of the hydrolytic product 4-nitrophenol as a function of time is obtained by measuring the UV/Vis absorbance as a function of time at 400 nm. Plots of the absorbance as a function of time are given in Figure S9 for pH 9.0 at different VK2H concentrations; the initial hydrolytic rate is obtained from the slope at zero time. In Figure 3B we plot the initial catalytic rate (v) relative to the rate at pH 9.5, as a function of increasing pH of the reaction buffer from 5.3 to 9.5. Below pH 7, almost no activity was recorded. From pH 7–9.5, the relative rate increases dramatically, which coincides with the formation of the fibril structure and supports the hypothesis that a catalytic microenvironment is formed by the fibril architecture of VK2H for the hydrolysis of pNPA. The equivalent catalytic experiments with VK2G showed much reduced catalytic activity, highlighting the importance of histidine to the catalysis (Figure S10A). VR2H serves as a control to assess the importance of the self-assembled state. At pH 9.0 this peptide shows negligible catalytic activity, comparable with that of histidine amide, indicating the critical role for self-assembly in forming an effective catalytic microenvironment (Figure S10).

Having demonstrated that both the self-assembly and the catalytic activity can be controlled by the pH, we investigated the switchable ability of the catalytic activity by alternating the pH multiple times. A stock solution (10 mL) of peptide VK2H at pH 6.0 was prepared and 500 μL was withdrawn and added into the cuvette, and the enzymatic activity was measured after adding pNPA. NaOH was then added to the stock to adjust the pH to alkaline; 500 μL of this pH 9.0 solution was withdrawn, and its activity was tested. Acid was subsequently added to the stock to reduce the pH back to 6.0, and a 500 μL aliquot was removed and tested for activity again. This cycle (pH 6, 9, 6) was then repeated multiple times. The results are shown in Figure 3C which plots the initial reaction rate as a function of cycle and demonstrates that the catalytic activity is completely reversible after multiple pH change cycles.

From the data for the initial rate of reaction (v) we can calculate the kinetic rate constants for VK2H fibrils and compare them with literature values for the hydrolytic activity of other artificial esterases derived from self-assembled structures. The initial rates of hydrolysis of pNPA catalyzed by VK2H at 9.0 in 15 mM Tris-HCl buffer were measured by varying the concentration of pNPA while fixing the concentration of VK2H. The double-reciprocal plots of the initial rate versus substrate concentration (1/[S]) (Figure 3D), are linear, indicating Michaelis–Menten kinetics with apparent kinetic constants, $k_{cat} = 0.07\ s^{-1}$, $K_M = 3.65$ (mM) and the efficiency, $k_{cat}/K_M = 19.18\ s^{-1}M^{-1}$. Compared to the previously reported artificial peptide-based hydrolases,[8] VK2H has amongst the highest efficiencies,[7] and about a third the value of the best performing catalytic amyloid which includes a metal in its catalytic center[6b] (Table S1).

Attractive features of the VK2H construct are that it can form hydrogels and that the phase behavior can be reversibly controlled from fluid to gel by change in pH. We confirm here that VK2H fibrils in the cross-linked and entangled hydrogel state retain the catalytic activity. A gelling solution of VK2H at pH 9.5 is prepared at 1.0 wt% (4.0 mM), and allowed to gel in an open vial. A 10 μL aliquot of substrate pNPA (500 μM) is added into the hydrogel. After a few seconds, the gel turned the distinctive yellow color of the chromogen 4-nitrophenol, indicating that the fibrils within the hydrogel were catalytically active. A similar experiment undertaken at pH 6 with the VK2H in the fluid phase showed no yellow color (Figure 4A). A more quantitative measure of the catalytic activity in the gel phase was undertaken by forming the gel directly in a cuvette, adding the substrate aliquot, and measuring the absorbance at 400 nm. The result (Figure 4D) demonstrates the rapid increase in absorbance. For comparison, the same solution volume of VK2H but at pH 6 showed only a very small increase in absorbance indicating little catalytic activity. These results show clearly that the VK2H hydrolase can be used to catalytically convert substrate to product with the peptide incorporated as a rigid monolith, which should prove useful in applications, for example in food related biotransformations, where catalytic activity can be temporally regulated and product can be easily separated by gel-to-solution transition.

In this study, we have successfully developed a pH switchable artificial hydrolase based on regulating the conformation of a self-assembling β-hairpin amphiphilic oligopeptides with a hydrolytically active residue at the N-terminus of the peptide. This model is efficient and switchable. In accordance with the MAX peptides[9e] histidine residues are expected to be exposed on the edge of the fibril in an ordered arrangement which, along with the hydrophobic edge (catalytic microenvironment), providing a site for binding of the substrate through hydrophobic interaction. The conformation of VK2H can be controlled by the pH, and that the catalytic activity follows the self-assembly "switch" with the unassembled random coils catalytically inactive and the fibrils able to catalyze the hydrolysis of substrate. The measured catalytic efficiency is in line with the best performing previously reported artificial hydrolases developed from self-assembled peptides, and these other constructs are not switchable. Finally, at high concentrations, the fibrils entangle and crosslink to form a hydrogel which also demonstrates strong catalytic active and provides the starting point for applications in which a hydrogel monolith can be used for enzymatic hydrolysis and the product recovered in a liquid phase by disassembling the gel.

Acknowledgements

This work was financially supported in part by grants from the CUNY ASRC Cooperative Postdoc Research Grant 2015, NSF-CBET 1512458 and the U.S. Army Research Laboratory

and the U.S. Army Research Office under contract/grant W911NF-16-1-0113.

Conflict of interest

The authors declare no conflict of interest.

Keywords: artificial hydrolase · peptide · self-assembly · pH-switch

How to cite: *Angew. Chem. Int. Ed.* **2017**, *56*, 14511 – 14515
Angew. Chem. **2017**, *129*, 14703 – 14707

[1] a) R. F. Goldberger, *Science* **1974**, *183*, 810 – 816; b) Z. R. Zhang, S. Perrett, *J. Biol. Chem.* **2009**, *284*, 14058 – 14067.
[2] a) N. M. Goodey, S. J. Benkovic, *Nat. Chem. Biol.* **2008**, *4*, 474 – 482; b) H. N. Motlagh, J. O. Wrabl, J. Li, V. J. Hilser, *Nature* **2014**, *508*, 331 – 339.
[3] a) O. V. Makhlynets, E. A. Raymond, I. V. Korendovych, *Biochemistry* **2015**, *54*, 1444 – 1456; b) C. Zhang, T. Pan, C. Salesse, D. Zhang, L. Miao, L. Wang, Y. Gao, J. Xu, Z. Dong, Q. Luo, J. Liu, *Angew. Chem. Int. Ed.* **2014**, *53*, 13536 – 13539; *Angew. Chem.* **2014**, *126*, 13754 – 13757.
[4] a) T. Shimoboji, E. Larenas, T. Fowler, S. Kulkarni, A. S. Hoffman, P. S. Stayton, *Proc. Natl. Acad. Sci. USA* **2002**, *99*, 16592 – 16596; b) T. Shimoboji, E. Larenas, T. Fowler, A. S. Hoffman, P. S. Stayton, *Bioconjugate Chem.* **2003**, *14*, 517 – 525.
[5] a) V. Blanco, D. A. Leigh, V. Marcos, *Chem. Soc. Rev.* **2015**, *44*, 5341 – 5370; b) J. Li, C. Si, H. Sun, J. Zhu, T. Pan, S. Liu, Z. Dong, J. Xu, Q. Luo, J. Liu, *Chem. Commun.* **2015**, *51*, 9987 – 9990.
[6] a) A. J. Burton, A. R. Thomson, W. M. Dawson, R. L. Brady, D. N. Woolfson, *Nat. Chem.* **2016**, *8*, 837 – 844; b) C. M. Rufo, Y. S. Moroz, O. V. Moroz, J. Stohr, T. A. Smith, X. Hu, W. F. DeGrado, I. V. Korendovych, *Nat. Chem.* **2014**, *6*, 303 – 309; c) T. O. Omosun, M. C. Hsieh, W. S. Childers, D. Das, A. K. Mehta, N. R. Anthony, T. Pan, M. A. Grover, K. M. Berland, D. G. Lynn, *Nat. Chem.* **2017**, DOI: https://doi.org/10.1038/nchem.2738; d) Y. Gao, F. Zhao, Q. Wang, Y. Zhang, B. Xu, *Chem. Soc. Rev.* **2010**, *39*, 3425 – 3433; e) Z. Huang, Q. Luo, S. Guan, J. Gao, Y. Wang, B. Zhang, L. Wang, J. Xu, Z. Dong, J. Liu, *Soft Matter* **2014**, *10*, 9695 – 9701; f) O. V. Makhlynets, P. M. Gosavi, I. V. Korendovych, *Angew. Chem. Int. Ed.* **2016**, *55*, 9017 – 9020; *Angew. Chem.* **2016**, *128*, 9163 – 9166.
[7] a) M. O. Guler, S. I. Stupp, *J. Am. Chem. Soc.* **2007**, *129*, 12082 – 12083; b) C. Zhang, X. Xue, Q. Luo, Y. Li, K. Yang, X. Zhuang, Y. Jiang, J. Zhang, J. Liu, G. Zou, X. J. Liang, *ACS Nano* **2014**, *8*, 11715 – 11723; c) Z. P. Huang, S. W. Guan, Y. G. Wang, G. N. Shi, L. N. Cao, Y. Z. Gao, Z. Y. Dong, J. Y. Xu, Q. Luo, J. Q. Liu, *J. Mater. Chem. B* **2013**, *1*, 2297 – 2304; d) A. M. Garcia, M. Kurbasic, S. Kralj, M. Melchionna, S. Marchesan, *Chem. Commun.* **2017**, DOI: https://doi.org/10.1039/C7CC03371K; e) N. Singh, M. P. Conte, R. V. Ulijn, J. F. Miravet, B. Escuder, *Chem. Commun.* **2015**, *51*, 13213 – 13216; f) M. Tena-Solsona, J. Nanda, S. Diaz-Oltra, A. Chotera, G. Ashkenasy, B. Escuder, *Chem. Eur. J.* **2016**, *22*, 6687 – 6694; g) M. P. Friedmann, V. Torbeev, V. Zelenay, A. Sobol, J. Greenwald, R. Riek, *PLoS One* **2015**, DOI: https://doi.org/10.1371/journal.pone.0143948.
[8] K. L. Duncan, R. V. Ulijn, *Biocatalysis* **2015**, *1*, 67 – 81.
[9] a) J. P. Schneider, D. J. Pochan, B. Ozbas, K. Rajagopal, L. Pakstis, J. Kretsinger, *J. Am. Chem. Soc.* **2002**, *124*, 15030 – 15037; b) K. Rajagopal, B. Ozbas, D. J. Pochan, J. P. Schneider, *Eur. Biophys. J.* **2006**, *35*, 162 – 169; c) L. Haines-Butterick, K. Rajagopal, M. Branco, D. Salick, R. Rughani, M. Pilarz, M. S. Lamm, D. J. Pochan, J. P. Schneider, *Proc. Natl. Acad. Sci. USA* **2007**, *104*, 7791 – 7796; d) D. A. Salick, D. J. Pochan, J. P. Schneider, *Adv. Mater.* **2009**, *21*, 4120 – 4123; e) K. Nagy-Smith, E. Moore, J. Schneider, R. Tycko, *Proc. Natl. Acad. Sci. USA* **2015**, *112*, 9816 – 9821.
[10] Y. Miller, B. Ma, R. Nussinov, *J. Phys. Chem. B* **2015**, *119*, 482 – 490.
[11] W. C. Johnson, Jr., *Annu. Rev. Biophys. Biophys. Chem.* **1988**, *17*, 145 – 166.

Manuscript received: August 6, 2017
Revised manuscript received: September 20, 2017
Accepted manuscript online: September 22, 2017
Version of record online: October 11, 2017

